

# Is the Birth of PSR J0538+2817 Accompanied by a Gamma-ray Burst?

Fan Xu,<sup>1</sup> Jin-Jun Geng,<sup>2</sup> Xu Wang,<sup>1</sup> Liang Li<sup>3</sup> and Yong-Feng Huang<sup>1,4\*</sup>

<sup>1</sup>*School of Astronomy and Space Science, Nanjing University, Nanjing 210023, People's Republic of China*

<sup>2</sup>*Purple Mountain Observatory, Chinese Academy of Sciences, Nanjing 210023, People's Republic of China*

<sup>3</sup>*ICRANet, Piazza della Repubblica 10, I-65122 Pescara, Italy*

<sup>4</sup>*Key Laboratory of Modern Astronomy and Astrophysics (Nanjing University), Ministry of Education, People's Republic of China*

Accepted XXX. Received YYY; in original form ZZZ

## ABSTRACT

Recently, the Five-hundred-meter Aperture Spherical radio Telescope (FAST) measured the three-dimensional velocity of PSR J0538+2817 in its associated supernova remnant S147 and found a possible spin-velocity alignment in this pulsar. Here we show that the high velocity and the spin-velocity alignment in this pulsar can be explained by the so-called electromagnetic rocket mechanism. In this framework, the pulsar is kicked in the direction of the spin axis, which naturally explains the spin-velocity alignment. We scrutinize the evolution of this pulsar and show that the pulsar kick can create a highly relativistic jet at the opposite direction of the kick velocity. The lifetime and energetics of the jet is estimated. It is argued that the jet can generate a Gamma-ray Burst (GRB). The long term dynamical evolution of the jet is calculated. It is found that the shock radius of the jet should expand to about 32 pc at present, which is well consistent with the observed radius of the supernova remnant S147 ( $32.1 \pm 4.8$  pc). Additionally, our calculations indicate that the current velocity of the GRB remnant should be about 440 km s<sup>-1</sup>, which is also consistent with the observed blast wave velocity of the remnant of S147 (500 km s<sup>-1</sup>).

**Key words:** gamma-ray bursts – stars: neutron – pulsars: general – stars: magnetars

## 1 INTRODUCTION

It is well known that many pulsars possess large velocities compared with main sequence stars. Recent statistical study of young pulsars has shown an average three-dimensional (3D) velocity of about 400 km s<sup>-1</sup> at birth (Hobbs et al. 2005). Some of the fastest ones can even reach  $\sim 1000$  km s<sup>-1</sup>. The origin of the high-velocity pulsars is still under debate. A natural requirement is kind of asymmetry during the supernova explosion that creates a kick to the pulsar. It has been suggested that an anisotropic mass ejection or neutrino ejection could be responsible for the pulsar kick (Sagert & Schaffner-Bielich 2008; Janka 2017). Meanwhile, the electromagnetic rocket mechanism is also a promising model to explain the high-velocity pulsars (Harrison & Tademaru 1975; Lai et al. 2001; Huang et al. 2003). In this framework, the young pulsar is supposed to have an off-centered dipolar magnetic field. The asymmetry in the magnetic field will lead to extra radiation in the direction of the spin axis and give the pulsar a recoil velocity. The timescale of the electromagnetic rocket process may last for a relatively long time (Janka et al. 2021). However, the timescale could also be as short as  $\sim 50$  s if the pulsar has a large magnetic field and a small initial period, namely a millisecond magnetar (Huang et al. 2003).

Recently, Yao et al. (2021) reported the evidence for 3D spin-velocity alignment of PSR J0538+2817. They adopted a scintillation method to get the radial velocity of this pulsar by using the observations made with the Five-hundred-meter Aperture Spherical Radio Telescope (FAST). Combining the pulsar observations of Chatterjee

et al. (2009), they derived the inclination angle between the pulsar 3D velocity and the line of sight as  $\zeta_v = 110^\circ +^{16}_-29^\circ$  and the overall 3D speed as  $407^{+79}_{-57}$  km s<sup>-1</sup>. Using the polarization fitting method, they further obtained the inclination angle of the pulsar spin axis with respect to the line of sight as  $\zeta_{pol} = 118^\circ.5 \pm 6.3^\circ$ . They argued that PSR J0538+2817 is the first pulsar that directly shows a 3D spin-velocity alignment. It is worth noting that the spin-velocity alignment has previously been hinted in the Crab and Vela pulsars, but observations only limit their alignments in the two-dimensional (2D) plane (Lai et al. 2001; Johnston et al. 2005). The 3D spin-velocity alignment is not easy to be explained by current simulations of supernova explosions which mainly focus on anisotropic mass ejection or neutrino ejection (Janka 2017; Müller et al. 2019). Recently, Janka et al. (2021) described a subtle scenario to explain the alignment, considering the asymmetric mass ejection in the supernova explosion. In all previous hydro-dynamical supernova simulations, the effect of accretion by the neutron star is generally omitted. In their new scenario, the newly-born neutron star obtains a high-velocity through the anisotropic supernova explosion in the first few seconds and runs away from the explosion center. Then the spin direction of this neutron star would later be affected by the fallback materials mainly from the direction of neutron star motion, which may potentially lead to some kinds of spin-velocity alignment. However, even in their simulations, a satisfactory alignment could be obtained only in some rare cases. On the other hand, we note that the spin-velocity alignment is a natural result in the framework of the electromagnetic rocket scenario (Harrison & Tademaru 1975). Thus we will mainly focus on this mechanism in our paper.

\* E-mail: hyf@nju.edu.cn

Gamma-ray Bursts (GRBs) are explosions with an extremely high

energy release. It is generally believed that long GRBs lasting for tens of seconds are associated with core collapse of massive stars (Woosley 1993; Iwamoto et al. 1998). Meanwhile, short GRBs lasting for less than  $\sim 2$  s are deemed to be related to the mergers of two compact stars (Eichler et al. 1989; Abbott et al. 2017). In the former scenario, the core collapse of massive stars often leaves a remnant of a black hole or a millisecond magnetar to act as the central engine of GRBs. However, as suggested by Dar & Plaga (1999), GRBs might also come from pulsar kicks. This model interestingly connects high-speed pulsars with GRBs. Later, Huang et al. (2003) examined the kick process and studied the properties of the resultant GRBs in details. Here, we go further to argue that the observed spin-velocity alignment of PSR J0538+2817 indicates that the birth of this pulsar may be associated with a long GRB.

This paper is organized as follows. In Section 2, we briefly introduce the observed features of PSR J0538+2817 and its associated supernova remnant (SNR) S147. Section 3 describes the GRB model in detail. We calculate the dynamics and compare our results with the observational data in Section 4. The possible decay of the magnetic field and the spin evolution of the pulsar is studied in Section 5. Finally, our conclusions and brief discussion are presented in Section 6.

## 2 PSR J0538+2817 AND S147

PSR J0538+2817 was first discovered by Anderson et al. (1996) with the Arecibo radio telescope. This pulsar is thought to be associated with SNR S147. It has a short period of 143.16 ms with a period derivative of  $3.67 \times 10^{-15} \text{ s s}^{-1}$  (Anderson et al. 1996; Kramer et al. 2003). Considering a simple magnetic dipole radiation, the characteristic age of this pulsar would be approximately 600 kyr. As for the distance, both parallax distance and the dispersion measure (DM) distance suggest that this pulsar is about 1.3 kpc away from us (Kramer et al. 2003; Chatterjee et al. 2009). The proper motion precisely measured by the Very Long Baseline Array (VLBA) of  $\mu_\alpha = -23.57 \pm 0.1 \text{ mas yr}^{-1}$  and  $\mu_\delta = 52.87 \pm 0.1 \text{ mas yr}^{-1}$  suggests a transverse velocity of  $357_{-43}^{+59} \text{ km s}^{-1}$  (Chatterjee et al. 2009). After converting it to the local standard of rest (LSR), the proper motion becomes  $\mu_\alpha = -24.4 \pm 0.1 \text{ mas yr}^{-1}$  and  $\mu_\delta = 57.2 \pm 0.1 \text{ mas yr}^{-1}$  (Dinçel et al. 2015). Then, assuming a distance of  $1.33 \pm 0.19$  kpc, the transverse velocity in the LSR is  $391 \pm 56 \text{ km s}^{-1}$  (Yao et al. 2021). From the transverse velocity and the conjecture of its association with S147, its kinematic age can be derived as  $34.8 \pm 0.4$  kyr (Yao et al. 2021). In general, we summarize the observed and derived parameters of PSR J0538+2817 in Table 1 for reference.

The kinematic age derived above is very different from the characteristic age of PSR J0538+2817. It indicates that the characteristic age may have been overestimated. Such an overestimation is not rare for pulsars and it may be caused by a variety of factors. For example, the magnetic field of pulsars may vary or decay on a long timescale (Guseinov et al. 2004). Another possibility is that the pulsar may have a large initial period. However, in the case of PSR J0538+2817, the initial period should be as long as  $P_0 = 139$  ms to make the two ages compatible (Kramer et al. 2003). Such a long initial period is very rare for young pulsars. In fact, it is widely believed that pulsars should be born with a millisecond initial period. In this study, we argue that PSR J0538+2817 should be a millisecond magnetar at birth. It will be shown below that the observed high speed and the spin-velocity alignment can all be naturally explained in this circumstance. The inconsistency between the kinematic age and the characteristic age is then attributed to a significant decay of

the dipolar magnetic field due to fallback accretion, which will be discussed in detail in Section 5.

As for the SNR of S147, although an early estimation gave a large age of about 100 kyr (Kirshner & Arnold 1979), it is often thought to have a smaller age of about 30 kyr, similar to the kinematic age of PSR J0538+2817 (Katsuta et al. 2012). Despite of its old age, this SNR still shows long delicate filaments in optical band with a nearly spherical shape (Dinçel et al. 2015). However, other than considering it as a perfect spherical shape, some authors argued that there exists an ‘‘ear’’ morphology in this SNR (Grichener & Soker 2017; Bear & Soker 2018). More interestingly, from the  $H\alpha$  image of S147 presented by Gvaramadze (2006), the filamentary structure seems to be more concentrated in the south-east, opposite to the direction of the pulsar proper motion. The distance of this remnant is estimated to be approximately 1.3 kpc, consistent with that of PSR J0538+2817 (Dinçel et al. 2015; Yao et al. 2021). Sofue et al. (1980) presented a 5 GHz map of S147 and measured its angular radius as  $\theta_s = 83' \pm 3'$ , which corresponds to a size of  $R_s = 32.1 \pm 4.8$  pc at a distance of  $1.33 \pm 0.19$  kpc (Yao et al. 2021).

The possible spin-velocity alignment of PSR J0538+2817 was previously proposed by Romani & Ng (2003). With the help of Chandra X-ray Observatory (CXO) imaging, they found that this pulsar might be surrounded by a faint pulsar wind nebula (PWN). Assuming that the elongated structure is an equatorial torus, they argued that the pulsar spin and velocity are aligned. This alignment was later supported by several other papers (Ng et al. 2007; Johnston et al. 2007), but only in the 2-dimensional plane. Recently, Yao et al. (2021) confirmed this alignment in the 3D space. They analyzed the scintillation arcs of PSR J0538+2817 based on the dynamic spectra obtained with FAST. Assuming that this pulsar is associated with S147 and that S147 has a spherical structure, they speculated that the pulsar-scattering screen is located at the SNR shell and determined the location of this pulsar in the 3D space. Then, considering the pulsar’s kinematic age, they derived the 3D velocity of the pulsar as  $407_{-57}^{+79} \text{ km s}^{-1}$  and the corresponding 3D inclination angle as  $\zeta_v = 110_{-29}^{+16} \text{ }^\circ$ . Also, they fitted the FAST polarization data with the rotating vector model (RVM) (Johnston et al. 2005) and got the inclination angle of the spin axis with respect to the line of sight as  $\zeta_{pol} = 118.5 \pm 6.3 \text{ }^\circ$ . These data strongly support the idea that the spin and velocity of PSR J0538+2817 are aligned.

## 3 GRB CONNECTED WITH THE BIRTH OF PSR J0538+2817

We argue that PSR J0538+2817 is born as a millisecond magnetar. At its birth, the electromagnetic rocket mechanism can satisfactorily explain the high kick speed and the spin-velocity alignment. In this framework, the kick of the pulsar should be accompanied by a relativistic jet moving in the opposite direction of the pulsar velocity. The jet will possess enough energy to power a long GRB. A schematic illustration of our scenario is shown in Figure 1. Here we describe the scenario in detail and confront our model with the various observational data.

### 3.1 Kick velocity and kick timescale

A pulsar with an off-centered dipolar magnetic field will lose energy asymmetrically, which would in return exert a recoil force on this pulsar (Harrison & Tademaru 1975). The force is parallel to the spin axis when averaged over a period. Therefore, the pulsar would acquire a kick velocity aligned to the spin axis.

**Table 1.** Parameters of PSR J0538+2817

Observed parameters	Value	Ref. <sup>a</sup>	Derived parameters	Value	Ref.
R.A. (J2000)	05 <sup>h</sup> 38 <sup>m</sup> 25.0623 <sup>s</sup>	2	Characteristic age (kyr)	600	4
Dec. (J2000)	28° 17' 09.1"	2	Kinematic age (kyr)	34.8±0.4	4
Period, $P$ (ms)	143.157776645(2)	1	DM distance, $D_{\text{DM}}$ (kpc)	1.2	3
First derivative, $\dot{P}$ ( $\times 10^{-15}$ )	3.6681(1)	1	Parallax distance, $D_{\pi}$ (kpc)	1.30 <sup>+0.22</sup> <sub>-0.16</sub>	3
Dispersion measure (pc cm <sup>-3</sup> )	39.57	3	Transverse velocity, $V_{\perp}$ (km s <sup>-1</sup> )	357 <sup>+59</sup> <sub>-43</sub>	3
$\mu_{\alpha}$ (mas yr <sup>-1</sup> )	-23.57 <sup>+0.10</sup> <sub>-0.10</sub>	3	3D velocity, $V_{3\text{D}}$ (km s <sup>-1</sup> )	407 <sup>+79</sup> <sub>-57</sub>	4
$\mu_{\delta}$ (mas yr <sup>-1</sup> )	52.87 <sup>+0.09</sup> <sub>-0.10</sub>	3	Magnetic field (G)	7 × 10 <sup>11</sup>	1
$\pi$ (mas)	0.72 <sup>+0.12</sup> <sub>-0.09</sub>	3	Spin-down luminosity (erg s <sup>-1</sup> )	5 × 10 <sup>34</sup>	1

<sup>a</sup> List of references: 1 - Anderson et al. (1996); 2 - Kramer et al. (2003); 3 - Chatterjee et al. (2009); 4 - Yao et al. (2021)

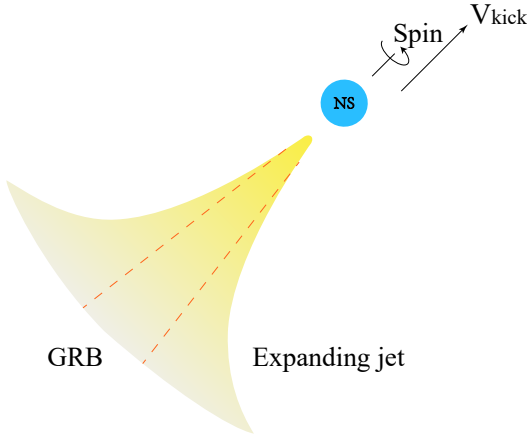


**Figure 1.** Schematic illustration of our scenario. The pulsar is born as a millisecond magnetar and gains a large kick velocity through the electromagnetic rocket process which lasts for approximately 180 s. Meanwhile, a highly beamed ultra-relativistic outflow is launched opposite to the kick direction, which will be powerful enough to generate a GRB. After producing the GRB, the jet continues to move outward, expanding laterally at the same time. After about 34.8 kyr, the radius of the jet increases to  $\sim 32$  pc, which is consistent with the observed radius of SNR S147 ( $32.1 \pm 4.8$  pc).

The kick speed  $V_{\text{kick}}$  depends on the exact configuration of the off-centered dipolar magnetic field. Here we consider a relatively simple case that the dipole is displaced by a distance of  $s$  with respect to the rotation axis. The dipole has a zero radial magnetic momentum of  $\mu_r = 0$  and a non-zero tangential momentum with  $\mu_z = 1.5\mu_{\phi}$ . Following Lai et al. (2001), we obtain the acquired kick velocity as

$$V_{\text{kick}} \simeq 445 \left( \frac{R}{12 \text{ km}} \right)^2 \left( \frac{P_0}{1 \text{ ms}} \right)^{-3} \left( \frac{s}{7 \text{ km}} \right) \left( \frac{\mu_z/\mu_{\phi}}{1.5} \right) \times \left[ 1 - \left( \frac{P_1}{P_0} \right)^{-3} \right] \text{ km s}^{-1}, \quad (1)$$

where  $R_{\text{NS}}$  is the radius of the pulsar,  $P_0$  and  $P_1$  are the initial period and the final period after the kick process respectively. We see that with typical parameters of  $R_{\text{NS}} = 12$  km,  $s = 7$  km and  $P_0 = 1$  ms, the kick speed can be larger than  $\sim 400$  km s<sup>-1</sup>.

During the kick process, the pulsar will lose energy and will correspondingly spin down (Harrison & Tademaru 1975). As a result, its period will evolve with time as,

$$P(t) \simeq P_0 \left[ 2.0 \times 10^{-2} \text{ s}^{-1} \left( \frac{P_0}{1 \text{ ms}} \right)^{-2} \left( \frac{R_{\text{NS}}}{12 \text{ km}} \right)^4 \left( \frac{\mu_z/\mu_{\phi}}{1.5} \right)^{-2} \times \left( \frac{B_0}{7 \times 10^{15} \text{ G}} \right)^2 t + 1 \right]^{\frac{1}{2}}, \quad (2)$$

where  $B_0$  is the surface magnetic field of the pulsar. Here we take the magnetic field as several times  $10^{15}$  G in our modeling, which is quite typical for a newborn millisecond pulsar (Metzger et al. 2011).

From Equation 1 and Equation 2, we see that the velocity acquired by the pulsar is a function of  $t$ . Taking  $V_{\text{kick}} \sim 400$  km s<sup>-1</sup> as a target speed, we find that the kick process will last for a timescale of  $\tau \sim 180$  s. After the kick process, the period of this pulsar decreases to  $P_1 = 2.15$  ms according to Equation 2.

### 3.2 Energetics of the GRB

Accompanying the kick, a jet will be launched due to the momentum conservation. The momentum of the jet can be calculated as  $P_{\text{flow}} = M_{\text{NS}} V_{\text{kick}}$ . In the electromagnetic rocket mechanism, very few baryons will be included in the jet, so that the outflow should be highly relativistic. Taking  $V_{\text{kick}} \sim 400$  km s<sup>-1</sup>, the total energy of the relativistic jet  $E_{\text{flow}}$  can be derived as (Dar & Plaga 1999; Huang et al. 2003)

$$E_{\text{flow}} = P_{\text{flow}} c = 3.3 \times 10^{51} \text{ erg} \times \left( \frac{M_{\text{NS}}}{1.4 M_{\odot}} \right) \left( \frac{V_{\text{kick}}}{400 \text{ km s}^{-1}} \right), \quad (3)$$

where  $c$  is the speed of light. Note that this pulsar is a millisecond magnetar at birth and the total energy of the jet should be smaller than the initial spin energy of the magnetar. Considering a typical moment of inertia of  $I = 10^{45}$  g cm<sup>2</sup>, the spin energy is

$$E_{\text{spin}} = \frac{1}{2} I \left( \frac{2\pi}{P_0} \right)^2 \approx 2 \times 10^{52} \left( \frac{I}{10^{45} \text{ g cm}^2} \right) \left( \frac{P_0}{1 \text{ ms}} \right)^{-2} \text{ erg}. \quad (4)$$

From the calculation in the above subsection, we get the terminal spin period after the kick process as  $P_1 = 2.15$  ms. It corresponds to a spin energy of  $E'_{\text{spin}} = 4.3 \times 10^{51}$  erg. There, the spin energy loss is  $\sim 1.57 \times 10^{52}$  erg. We see that this energy is large enough to energize the jet, thus the above kick process is basically self-consistent.

If observed on-axis, the jet will show up as a GRB. Usually only a portion of the kinetic energy will be emitted as  $\gamma$ -rays during the main burst phase. Designating the efficiency of  $\gamma$ -ray emission as  $\epsilon$  and the half opening angle of the jet as  $\theta$ , then the isotropic energy

of the GRB is

$$E_{\text{iso}} = \frac{2\varepsilon E_{\text{flow}}}{1 - \cos\theta} \approx 4\varepsilon M_{\text{NS}} V_{\text{NS}} c \theta^{-2} = 1.3 \times 10^{53} \text{ erg} \\ \times \left(\frac{\varepsilon}{0.1}\right) \left(\frac{\theta}{0.1}\right)^{-2} \left(\frac{M_{\text{NS}}}{1.4 M_{\odot}}\right) \left(\frac{V_{\text{NS}}}{400 \text{ km s}^{-1}}\right). \quad (5)$$

We see that for typical parameters of  $\varepsilon = 0.1$  and  $\theta = 0.1$ , the isotropic energy of the GRB can be as high as  $10^{53}$  erg. In our scenario, since the kick process lasts for  $\tau \sim 180$  s, the GRB should correspondingly be a long one.

#### 4 DYNAMICS OF THE REMNANT

The kick process and the accompanied GRB occurred about 34.8 kyr ago. After producing the  $\gamma$ -ray burst, the jet interacted with the circum-burst interstellar medium and got decelerated. It would expand laterally as well. Now we calculate the long-term dynamical evolution of the outflow and compare the results with the observational data of the remnant S147.

The dynamical evolution of relativistic outflows that produce GRBs has been extensively studied by many authors. Following the generic dynamical equation proposed by Huang et al. (1999), many other authors have studied some subtle effects such as the role played by the pressure of the shocked material (van Eerten et al. 2010; Pe'er 2012). Xu & Huang (2010) investigated the evolution of a ring-shaped jet. Lamb et al. (2018) studied the jet-cocoon interaction. Geng et al. (2013, 2016) discussed the effect of a delayed energy injection. Zouaoui & Mebarki (2019) examined the compatibility of the generic dynamical equation with the Sedov solution in the non-relativistic phase. Jet propagating through a density-jump medium (Geng et al. 2014) or a stratified circumstellar medium (Fraija et al. 2021) are also studied in detail. Very recently, magnetized GRB shocks have been further discussed by Chen & Liu (2021).

The case studied here is relatively simple. We only need to consider an adiabatic jet interacting with a homogeneous interstellar medium (ISM). Following Huang et al., the dynamics of the jet can be described by the following four equations (Huang et al. 1999, 2000a,b),

$$\frac{dR}{dt} = \beta c \gamma (\gamma + \sqrt{\gamma^2 - 1}), \quad (6)$$

$$\frac{dm}{dR} = 2\pi R^2 (1 - \cos\theta) n m_p, \quad (7)$$

$$\frac{d\theta}{dt} = \frac{c_s (\gamma + \sqrt{\gamma^2 - 1})}{R}, \quad (8)$$

$$\frac{d\gamma}{dm} = -\frac{\gamma^2 - 1}{M_{\text{ej}} + \varepsilon_r m + 2(1 - \varepsilon_r) \gamma m}. \quad (9)$$

Here,  $R$  is the radius of the shock in the GRB rest frame,  $m$  is the swept-up ISM mass,  $\gamma$  is the Lorentz factor of the outflow and  $\beta = \sqrt{\gamma^2 - 1}/\gamma$ ,  $t$  is the observer's time,  $n$  is the number density of the surrounding ISM,  $m_p$  is the proton's mass,  $c_s$  is the comoving sound speed, and  $\varepsilon_r$  is the radiative efficiency.

We have calculated the long-term evolution of the jet numerically. The parameters involved are taken as follows. Following our model described in Section 3, the total energy of the jet is  $E_{\text{flow}} = 3.3 \times 10^{51}$  erg. The mass of ejecta is set as  $M_{\text{ej}} = 1.2 \times 10^{-6} M_{\odot}$ , so that the initial Lorentz factor takes a typical value of  $\gamma_0 = 150$  ( $E_{\text{flow}} = \gamma_0 M_{\text{ej}} c^2$ ). The initial half opening angle of the jet is assumed as  $\theta_0 = 0.1$ . Considering that S147 is in a low-density area (Katsuta et al. 2012), we take the number density as  $n = 0.1 \text{ cm}^{-3}$ . The numerical result for the evolution of the shock radius is shown in Figure 2.

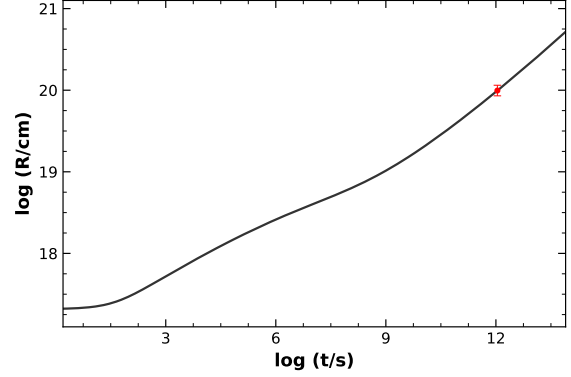


**Figure 2.** Long-term evolution of the shock radius after the jet produced the GRB. The observational data point represents the measured radius of S147 at present, which is  $32.1 \pm 4.8$  pc (Yao et al. 2021). The calculated shock radius is 32.04 pc after 34.8 kyr, which is well consistent with the observations.

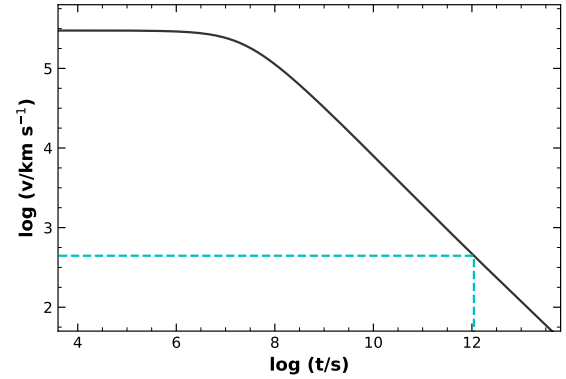


**Figure 3.** Long-term evolution of the shock velocity after the jet produced the GRB. The dashed lines mark the shock velocity at present, which is  $440 \text{ km s}^{-1}$ . It is consistent with the speed of  $\sim 500 \text{ km s}^{-1}$  estimated from observations by Katsuta et al. (2012).

We find that the shock radius of the jet is about 32.04 pc at present, which agrees well with the measured radius of S147 ( $32.1 \pm 4.8$  pc, at a distance of 1.33 kpc). Figure 3 illustrates the evolution of the shock velocity. S147 is currently in the Sedov-Taylor phase. Katsuta et al. (2012) have estimated its blast wave velocity as  $500 \text{ km s}^{-1}$ . As shown in Figure 3, our result indicates an expansion velocity of about  $440 \text{ km s}^{-1}$  for the remnant today. It is also well consistent with the estimation made by Katsuta et al. (2012).

#### 5 MAGNETIC FIELD DECAY AND PERIOD EVOLUTION

In our scenario, the initial magnetic field strength of this pulsar is  $B_0 = 7 \times 10^{15}$  G. However, the current surface field inferred from the period derivative is around  $7 \times 10^{11}$  G. It indicates that PSR J0538+2817 may have experienced a significant magnetic field decay.

Magnetic field decay has been frequently inferred from pulsar observations. A most recent example is the famous binary neutron



star merger event of GW170817. Although the possibility that the leftover after the merger is a black hole has not been completely expelled, many researchers believe that the remnant should be a massive neutron star (Yu et al. 2018). The remnant neutron star is thought to have an initial surface magnetic field of  $10^{14} - 10^{15}$  G. However, constraints from the data of later kilonova observations suggest that the field has decayed to  $10^{11} - 10^{12}$  G in a few thousands of seconds after the gravitational wave event (Yu et al. 2018). Some unknown mechanism has acted to significantly reduce the magnetic field.

How the magnetic field of neutron stars decays is still under debate. For isolated pulsars, maybe the most probable mechanism should involve Ohmic dissipation or Hall drift (Pons & Geppert 2007). However, this is not an effective process and the dissipation timescale usually lasts for about  $10^4 - 10^6$  yr (Pons & Geppert 2007). Another possibility is that the pulsar accretes matter which buries the magnetic field to make it decrease (Fu & Li 2013; Yu et al. 2018). The accreted matter can either from a companion star or from the fallback materials.

Here, for PSR J0538+2817, we adopt the latter mechanism and consider the fallback accretion. An empirical relationship between the magnetic field and the accreted mass ( $\Delta M$ ) can be written as (Shibazaki et al. 1989; Fu & Li 2013),

$$B = \frac{B_0}{1 + \Delta M / 10^{-5} M_{\odot}}, \quad (10)$$

where  $B_0$  is the initial magnetic field. For the magnetic field to decrease from  $B_0 = 7 \times 10^{15}$  G to the currently observed value of  $B = 7 \times 10^{11}$  G, the total accreted matter should be  $\Delta M \sim 10^{-1} M_{\odot}$ . Very recently, a detailed numerical simulation on the fallback accretion process has been conducted by Janka et al. (2021). It is revealed that a fallback mass of  $\Delta M \sim 10^{-1} M_{\odot}$  is quite typical in the process (Janka et al. 2021). Additionally, the accretion timescale is generally in the range of  $10^3 - 10^5$  s.

The decay of the magnetic field will have a significant influence on the spin-down of the pulsar. From our calculations in Section 3.1, we have argued that PSR J0538+2817 should have a small initial period of  $P_0 \sim 1$  ms (see Equation 1). Then it will experience an electromagnetic kick process that lasts for about  $\tau \sim 180$  s. After the kick process, the spin period decreases to about  $P_1 = 2.15$  ms (see Equation 2). Later, the pulsar will spin down through normal dipolar emission mechanism. At this stage, if the pulsar had a constant magnetic field of  $7 \times 10^{15}$  G, then the spin period would increase to about 370 ms in less than  $\sim 1 \times 10^6$  s. However, as argued above, the magnetic field actually decayed significantly on a timescale of  $\sim 10^3 - 10^5$  s due to the fallback accretion. Since the spin-down rate is proportional to the square of the surface magnetic field, the spin period will increase much slower. It would finally reach the observed period of 143 ms after 34.8 kyr. However, the detailed spin down process with a decreasing magnetic field is quite complicated and is beyond the scope of this study.

## 6 CONCLUSIONS AND DISCUSSION

An interesting spin-velocity alignment was recently reported for the high speed pulsar PSR J0538+2817 (Yao et al. 2021). We argue that this pulsar was initially born as a millisecond magnetar with a strong but asymmetrical magnetic field. The high kick speed and the spin-velocity alignment can be explained in the frame work of the electromagnetic rocket mechanism (Harrison & Tademaru 1975; Lai et al.

2001; Huang et al. 2003). It is suggested that the pulsar kick is accompanied by an ultra-relativistic jet in the opposite direction, which can essentially give birth to a long GRB. The long-term dynamical evolution of the jet is calculated. It is found that the shock radius of the jet should be 32.04 pc at present, which is well consistent with the observed radius of SNR S147 ( $32.1 \pm 4.8$  pc) (Yao et al. 2021). The current shock velocity from our result is about  $440 \text{ km s}^{-1}$ . It also agrees well with the estimated speed of  $\sim 500 \text{ km s}^{-1}$  by Katsuta et al. (2012).

In our model, an off-centered dipolar magnetic field is needed for PSR J0538+2817. Usually the magnetic field of pulsars is thought to be of a simple dipolar configuration which is not off-centered. However, note that the realistic situation might be much more complicated. For example, it has been suggested that the most rapidly rotating neutron stars may have more complex surface magnetic configuration (Ruderman et al. 1998). Meanwhile, recently Miller et al. (2019) studied PSR J0030+0451 and provided interesting constraints on its surface magnetic field from the hot spot observations. They used the observational data from the Neutron Star Interior Composition Explorer (*NICER*) and discerned three hot spots on the surface of the compact star. They argued that these hot spots strongly indicate that the pulsar has an offset dipolar magnetic field or even a multi-pole field. Therefore, for PSR J0538+2817, we believe that the existence of an off-centered magnetic field could not be expelled. In fact, the bulk magnetic field configuration of pulsars is closely connected with their internal structure. However, our knowledge about the interiors of neutron stars is still quite poor. For example, these so called ‘‘neutron stars’’ might even be strange quark stars (Geng et al. 2021). We hope that the unprecedented high accuracy observations of *NICER* on pulsars would help clarify the fascinating enigmas of neutron stars.

It has been shown that the kick process of PSR J0538+2817 might be accompanied by a GRB that happened in our own Galaxy about 30000 years ago. The filamentary structure of SNR S147 seems to be more concentrated in the south-east, opposite to the kick direction. This may support our model, where a jet produced the GRB is generated at the opposite direction of the kick. However, it is not clear whether this GRB pointed toward us. If it did point toward us, it would impose a huge effect to the Earth. Interestingly, in a recent work, Wang et al. (2017) measured the  $^{14}\text{C}$  abundance of an ancient buried tree. They found rapid increases of  $^{14}\text{C}$  in the tree rings between BC 3372 and BC 3371. They suggested that it may be associated with the ancient supernova that create the Vela pulsar. Similarly, we propose that people could also try to search for possible clues connected with the birth of PSR J0538+2817 about 34.8 kyr ago through geological surveys.

Observationally, the GRB rate is only  $\sim 0.2\%$  of the SN rate (Woosley & Bloom 2006). Meanwhile, high-velocity neutron stars are quite common, and the average velocity of pulsars is about  $400 \text{ km s}^{-1}$  at birth (Hobbs et al. 2005). One may worry that there would be too many GRBs according to our modeling. The contradiction can be relieved by considering the following requirements. First, not all high-speed pulsars are accompanied by an ultra-relativistic outflow. Some of them may acquire the high speed via other mechanisms. Second, the pulsar needs to be a millisecond one, together with a very strong magnetic field. Thirdly, even if the pulsar is accompanied by an ultra-relativistic outflow, the outflow may do not point toward us so that no GRB would be observed due to the beaming effect.

**ACKNOWLEDGEMENTS**

This work is supported by National SKA Program of China No. 2020SKA0120300, by the National Natural Science Foundation of China (Grant Nos. 11873030, 12041306, U1938201, 11903019, 11833003), and by the science research grants from the China Manned Space Project with NO. CMS-CSST-2021-B11.

**DATA AVAILABILITY**

This theoretical study did not generate any new data.

**REFERENCES**

- Abbott B. P., et al., 2017, *ApJ*, **848**, L13
- Anderson S. B., Cadwell B. J., Jacoby B. A., Wolszczan A., Foster R. S., Kramer M., 1996, *ApJ*, **468**, L55
- Bear E., Soker N., 2018, *ApJ*, **855**, 82
- Chatterjee S., et al., 2009, *ApJ*, **698**, 250
- Chen Q., Liu X.-W., 2021, *MNRAS*, **504**, 1759
- Dar A., Plaga R., 1999, *A&A*, **349**, 259
- Dinçel B., Neuhäuser R., Yerli S. K., Ankay A., Tetzlaff N., Torres G., Murgauer M., 2015, *MNRAS*, **448**, 3196
- Eichler D., Livio M., Piran T., Schramm D. N., 1989, *Nature*, **340**, 126
- Frajia N., Kamenetskaia B. B., Dainotti M. G., Duran R. B., Gálvan Gámez A., Dichiara S., Caligula do E. S. Pedreira A. C., 2021, *ApJ*, **907**, 78
- Fu L., Li X.-D., 2013, *ApJ*, **775**, 124
- Geng J. J., Wu X. F., Huang Y. F., Yu Y. B., 2013, *ApJ*, **779**, 28
- Geng J. J., Wu X. F., Li L., Huang Y. F., Dai Z. G., 2014, *ApJ*, **792**, 31
- Geng J. J., Wu X. F., Huang Y. F., Li L., Dai Z. G., 2016, *ApJ*, **825**, 107
- Geng J., Li B., Huang Y., 2021, *The Innovation*, **2**, 100152
- Granot J., Guetta D., Gill R., 2017, *ApJ*, **850**, L24
- Grichener A., Soker N., 2017, *MNRAS*, **468**, 1226
- Guseinov O. H., Ankay A., Tagieva S. O., 2004, *International Journal of Modern Physics D*, **13**, 1805
- Gvaramadze V. V., 2006, *A&A*, **454**, 239
- Harrison E. R., Tademaru E., 1975, *ApJ*, **201**, 447
- Hobbs G., Lorimer D. R., Lyne A. G., Kramer M., 2005, *MNRAS*, **360**, 974
- Huang Y. F., Dai Z. G., Lu T., 1999, *MNRAS*, **309**, 513
- Huang Y. F., Dai Z. G., Lu T., 2000a, *MNRAS*, **316**, 943
- Huang Y. F., Gou L. J., Dai Z. G., Lu T., 2000b, *ApJ*, **543**, 90
- Huang Y. F., Dai Z. G., Lu T., Cheng K. S., Wu X. F., 2003, *ApJ*, **594**, 919
- Iwamoto K., et al., 1998, *Nature*, **395**, 672
- Janka H.-T., 2017, *ApJ*, **837**, 84
- Janka H. T., Wongwathanarat A., Kramer M., 2021, arXiv e-prints, p. [arXiv:2104.07493](https://arxiv.org/abs/2104.07493)
- Johnston S., Hobbs G., Vigeland S., Kramer M., Weisberg J. M., Lyne A. G., 2005, *MNRAS*, **364**, 1397
- Johnston S., Kramer M., Karastergiou A., Hobbs G., Ord S., Wallman J., 2007, *MNRAS*, **381**, 1625
- Katsuta J., et al., 2012, *ApJ*, **752**, 135
- Kirshner R. P., Arnold C. N., 1979, *ApJ*, **229**, 147
- Kramer M., Lyne A. G., Hobbs G., Löhmer O., Carr P., Jordan C., Wolszczan A., 2003, *ApJ*, **593**, L31
- Lai D., Chernoff D. F., Cordes J. M., 2001, *ApJ*, **549**, 1111
- Lamb G. P., Mandel I., Resmi L., 2018, *MNRAS*, **481**, 2581
- Metzger B. D., Giannios D., Thompson T. A., Bucciantini N., Quataert E., 2011, *MNRAS*, **413**, 2031
- Miller M. C., et al., 2019, *ApJ*, **887**, L24
- Müller B., et al., 2019, *MNRAS*, **484**, 3307
- Ng C. Y., Romani R. W., Brisken W. F., Chatterjee S., Kramer M., 2007, *ApJ*, **654**, 487
- Pe'er A., 2012, *ApJ*, **752**, L8
- Pons J. A., Geppert U., 2007, *A&A*, **470**, 303
- Romani R. W., Ng C. Y., 2003, *ApJ*, **585**, L41

- Ruderman M., Zhu T., Chen K., 1998, *ApJ*, **492**, 267
- Sagert I., Schaffner-Bielich J., 2008, *A&A*, **489**, 281
- Shibazaki N., Murakami T., Shaham J., Nomoto K., 1989, *Nature*, **342**, 656
- Sofue Y., Furst E., Hirth W., 1980, *PASJ*, **32**, 1
- van Eerten H. J., Leventis K., Meliani Z., Wijers R. A. M. J., Keppens R., 2010, *MNRAS*, **403**, 300
- Wang F. Y., Yu H., Zou Y. C., Dai Z. G., Cheng K. S., 2017, *Nature Communications*, **8**, 1487
- Woosley S. E., 1993, *ApJ*, **405**, 273
- Woosley S. E., Bloom J. S., 2006, *ARA&A*, **44**, 507
- Xu M., Huang Y. F., 2010, *A&A*, **523**, A5
- Yao J., et al., 2021, *Nature Astronomy*, **5**, 788
- Yu Y.-W., Liu L.-D., Dai Z.-G., 2018, *ApJ*, **861**, 114
- Zouaoui E., Mebarki N., 2019, arXiv e-prints, p. [arXiv:1911.07350](https://arxiv.org/abs/1911.07350)

This paper has been typeset from a  $\text{\TeX}/\text{\LaTeX}$  file prepared by the author.